Available online at www.sciencedirect.com
ScienceDirect
International Journal of Heat and Mass Transfer 51 (2008) 4704–4716
International Journal of HEAT and MASS TRANSFER
www.elsevier.com/locate/ijhmt

Heat and mass transfer during drying of a bed of shrinking particles – Simulation for carrot cubes dried in a spout-fluidized-bed drier

Ireneusz Białobrzewski [a,*], Magdalena Zielińska [a], Arun S. Mujumdar [b], Marek Markowski [a]

[a] Department of Agri-Food Process Engineering, University of Warmia and Mazury, Heweliusza 14, 10-718 Olsztyn, Poland
[b] Department of Mechanical Engineering and Engineering Science Program, National University of Singapore, Singapore

Received 1 November 2007; received in revised form 12 February 2008
Available online 21 April 2008

Abstract

The purpose of the present study was to develop a model to describe the heat and mass transfer during the drying of carrot cubes in a spout-fluidized-bed drier. The model took into account the non-homogeneous shrinkage of the material. The Arbitrary Lagrange–Eulerian (ALE) formulation was applied to enter the problem with moving boundaries. Three phases of drying were distinguished according to the behavior of changes in percent local error of estimation: an initial phase of warming up the material – characterized by a low level of error of moisture content prediction, a second phase – characterized by an increase in the error of moisture content prediction and a phase of decreasing error. A simple test of the sensitivity of the model to the changes in heat transfer coefficient was performed in order to improve the ability of the model to predict the changes in moisture content and temperature of dried carrots. The predicted changes in both the moisture content and the temperature of carrot cubes during drying in a spout-fluidized-bed drier indicate that the model can be successfully applied to describe moisture content, temperature and deformation of dried particles in cases when the very high accuracy of moisture content and temperature prediction is not a crucial element of investigation of the drying process.

Keywords: Particulate material; Drying; Shrinkage; Heat and mass transfer; Mathematical modeling; ALE formulation

1. Introduction

Drying is an important method of preservation of wet materials and is applicable to a wide range of industrial and agricultural products, including foodstuffs. Various methods of drying have been developed for particulate materials, including fluidized-bed and spouted-bed drying techniques. Considering the thermal efficiencies of the drying process, fluidized bed dryers are extensively used in particulate foods drying because they ensure high intensities of heat and mass transfer [1] accompanied by high rates of drying. Fluidized-bed drying has found many applications in chemical, metallurgical and pharmaceutical industries. They have also been investigated as a potential method for obtaining high-quality dried foodstuffs, including fruit, vegetables and grain [2,3]. A combination of two distinct hydrodynamic regimes observed during particulate foods drying in a spouted-bed drier (pneumatic transport in the spout and a moving bed in the downcomer) permits uniform drying and minimizes the risk of material getting degraded [4]. Another option is to apply a spout-fluidized-bed drying technique which combines the main features of fluidized-bed and spouted-bed drying techniques [5].

Drying of biological materials, like fruit and vegetables, in a spouted or spout-fluidized bed is an extremely complicated process due to the simultaneous phenomena of heat, mass and momentum transfer which occurs inside each particle in the bed and transfer phenomena between solid and gas phases of the circulating bed being the mixture

* Corresponding author. Tel.: +48 89 523 45 81; fax: +48 89 523 44 69.
E-mail address: irekb@uwm.edu.pl (I. Białobrzewski).

0017-9310/$ - see front matter © 2008 Elsevier Ltd. All rights reserved.
doi:10.1016/j.ijheatmasstransfer.2008.02.031

Nomenclature

A, a, b, c	constants in equations, –
c_p	specific heat, J kg^{-1} K^{-1}
d_E	equivalent diameter of a solid, m
D	effective mass diffusion coefficient, m^2 s^{-1}
err	local percent error of estimation, %
h_m	mass transfer coefficient, m s^{-1}
h_T	heat transfer coefficient, W m^{-2} K^{-1}
k	turbulent energy, m^2 s^{-2}
L	dimensional characteristics (hydraulic diameter), m
M	moisture content of raw material dry basis, kg kg^{-1}
$\boldsymbol{n}$	direction normal to surface S, –
Nu	Nusselt number, –
P	pressure, Pa
Pr	Prandtl number, –
r	sorpion heat of pure water, J kg^{-1}
Re	Reynolds number, –
Sc	Schmitt number, –
Sh	Sherwood number, –
Simul	simulated value, –
t	time, s
T	temperature, °C
u	displacement of surface, m
$\mathbf{U}$	average velocity, m s^{-1}
X	moisture content of raw material (wet basis), –
$\boldsymbol{v}$	velocity of drying air, m s^{-1}
V_E	equivalent volume of a solid, m^3

Greek letters

λ	thermal conductivity, W m^{-1} K^{-1}
μ	viscosity, Pa s
ρ	density, kg m^{-3}
ε	dissipation rate of turbulence energy, m^2 s^{-3}

Subscripts

a	ambient
AB	gas phase
e	equillibrium
f	film
s	dry substance
S	surface of a body
w	water
0	initial value

of dried granulated material and air. Moreover, the particles of wet material undergo significant shrinkage which affects changes in both the shape and dimensions of the solid. Hot air drying of fruit and vegetables usually provokes changes in physical, chemical, nutritional and biological properties and modifies the characteristics of food products. In most cases these changes are dependent on moisture content, temperature and time of exposition.

An understanding of the transfer phenomena taking place during the drying of fruit and vegetables in rotating beds would result in the formulation of adequate mathematical models to optimize the process – leading to improved product quality and a reduction in process costs. Numerous analytical and numerical models have been proposed by various authors to study heat and moisture transfer analysis during drying of different solid objects. Reviews of several different mathematical models have been published [6,7]. In most cases, the authors employed the finite element method (FEM) for studying temperature and moisture distributions within the wet solids during the drying and control volume (CV) technique to study hydrodynamics and transfer phenomena in fluidized and spouted beds. All drying models described in the literature were derived under different simplifying assumptions, which strictly limit the application of these models.

One of the most common oversights in the modeling of the drying of solid foodstuffs is to neglect the shrinkage phenomenon. However, it should be underlined that one of the most important physical changes in the material that occurs during drying is the reduction of its external volume, in some cases also accompanied by changes in its shape. The above is caused by significant stresses affecting the cellular structure of the material being dried which occur when the moisture loss is significant and the material is anisotropic, which is the case during the drying of fruit and vegetables [8]. During the drying process, fruits and vegetables suffer great alterations to their original form (even up to 90%) due to significant shrinkage. The shrinkage phenomenon also affects the length of the diffusion path in dried material, influencing the moisture diffusion coefficient of the material and, as a result, influences the rate of drying. Knowledge of the shrinkage mechanism, and the influence of the process variables on shrinkage, will improve the understanding of drying kinetics. Therefore, as shrinkage in fruits and vegetables is an observable phenomenon, it must be taken into account in mathematical simulations of the drying process of these materials.

The evolution of deformation resulting in shrinkage of biological materials during drying, averaged over the volume of dried body and expressed as a function of water content, has been the subject of several studies. Most of the authors showed the linear shrinkage profile versus moisture content as a typical profile valid for fruit and vegetables [9,10] but others suggested an exponential or quadratic function to describe the shrinkage versus water content [8]. The most important disadvantage of the averaged shrinkage models which are usually applied for simulation is their inability to describe the local changes in the position of any given point inside a dried body. The ability of the shrinkage model to describe both the local values of

shrinkage vs. the local moisture content, as well as the drying time-dependent positions of any given point inside the dried material, is very important and enables the use of such a model for quality optimization of dried material.

Much research has been conducted in recent years to develop accurate mathematical models to simulate the behavior of heat and mass transfer processes and to define, over a wide range of drying conditions and different types of foods, the optimal set of operating conditions [4,6,11–15]. In most cases, the models developed had the ability to predict changes in temperature and moisture content in non-shrinking or homogeneously shrinking materials only. Therefore, the purpose of the present study was to develop a model describing the heat and mass transfer during the drying of particulate materials, taking into account the non-homogeneous shrinkage of the material. A bed of carrot cubes dried in a spout-fluidized-bed drier was used as the exemplary material. The Arbitrary Lagrange–Eulerian (ALE) formulation was applied to build the shrinkage model dependent on local moisture content of the material. The model was applied to describe changes in moisture content and temperature as well as in particle shape and dimensions during the drying of carrots. Extensive experiments were performed using cut carrots as a sample to compare the simulation and experimental results for validation purposes.

2. Mathematical model

Mathematical models describing flow of a mixture of a particulate material and a gas can be classified in two different categories. In a continuous model (Eulerian–Euleran formulation), particles of a solid phase are considered as a continuous phase, which is mixed with the gas phase. In such a formulation, the equations formulated for solid phase are in a form adequate for the continuous phase. Constitutive equations are usually built using not only the theory of mixtures, but also based on the kinetic theory of gases. The other option is the Lagrange–Eulerian formulation, in which solid particles are considered as a discrete phase. In this model, the gas phase is described with the equations as for fluids, while the motion of particles of a solid phase is described by Newton's second law of motion. If the concentration of particles is low, then it can be assumed that the motion of solid particles is determined by the velocity field of the gas phase and the particles do not disturb the motion of the gas. However, in the case of higher concentration of particulate material phase, the equations describing the motion of both phases contain terms describing the interfacial momentum exchange, which ensures the coupling of the motion of gas and solid phases.

The problem under investigation is the forced convection of the air through a wet spout-fluidized bed of carrot cubes circulating in the vertical cylinder. The solid phase of the bed is discontinuous. In a cylindrical-shaped fluidized bed, the solid phase is usually nearly-uniformly distributed in the bed. In a spouted bed, whose domain is the sum of a cone and a cylinder, several zones of different volume fractions of the solid phase are observed and the highest value of the volume fraction is usually concentrated at the bottom part of the bed [4]. In the spout-fluidized bed driers, the material is located only in the cylindrical part of the drying chamber. If the height of the static bed is lower than the diameter of a cylinder, then nearly all of the solid phase of the gas–solid mixture is distributed near the bottom of the cylinder with the maximum of the mass fraction of the solid phase of the mixture observed near the cylinder wall and minimum near its axis [5]. This can be seen in the schematic diagram of the spout-fluidized bed under investigation shown in Fig. 1.

Several assumptions are made in order to obtain a closed set of governing equations of heat and mass transfer in cut carrots:

- The motion of the solid particles in the mixture do not disturb the motion of the air phase, i.e. the concentration of the solid phase in the mixture can be neglected during simulation of the velocity field of the air inside the drying chamber. As a consequence of this assumption in the govern equations modeling air flow there are no mass, momentum, energy sources terms. That is, water vapor evaporated from carrots has negligible effect on the humidity and temperature of the drying air.
- The average velocity of the air flowing round a single solid particle in the mixture of particulate material and the air do not differ significantly from the velocity of the air simulated for the air flowing through the empty apparatus and averaged in that domain inside the drying chamber in which the dried material is located during drying (Fig. 1).
- A single particle being dried is the regular cube. Heat and mass transfer inside each particle is three-dimensional.
- Convection-type boundary conditions are valid for the drying of a single particle.

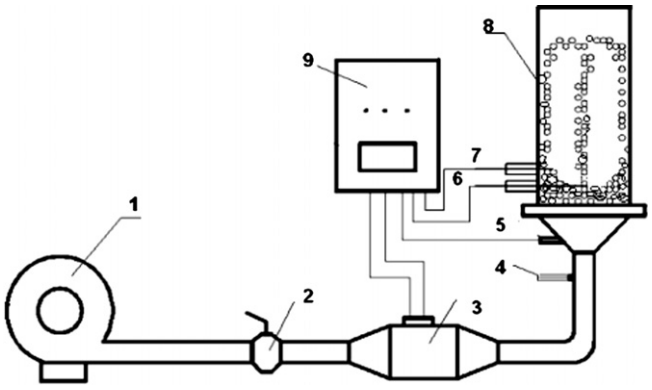

Fig. 1. Schematic diagram of the experimental apparatus: 1 – fan; 2 – air flow regulating valve; 3 – heaters; 4–7 – thermocouples, 8 – drying chamber, 9 – heat control unit.

- The initial distributions of moisture content and temperature inside each particle are uniform.
- Water evaporation takes place only at the surface of a particle.
- A particle of carrot to be dried is considered as a binary system containing solid and liquid phase components.
- Heat and mass transfer as shrinkage of dried particle are also interrelated.
- Shrinkage of a dried body can be described by an empirical model of changes in the volume of dried particle coupled with the theoretical model of displacement of its surface and interior.
- A dried particle shrinks, but its shape does not change during drying.

The macroscopic equations applied to describe simultaneous heat and mass transfer in a typical shrinking wet carrot cube subjected to convection boundary conditions were applied and written in 3D Cartesian coordinates, which were fixed in the geometric center of the cube.

2.1. Air flow distribution

Computer simulations were performed to determine the average relative velocity of the air flow around a single solid particle during drying in the mixture of carrot cubes and the air flow through the empty drying chamber. The simulations were performed using continuity and momentum equations in the form (1)–(7). The standard κ–ε dispersed turbulence model was used during simulations

$$\nabla \cdot \mathbf{U} = 0, \tag{1}$$

$$\rho \frac{\partial \mathbf{U}}{\partial t} - \nabla \cdot \left[\left(\mu + \rho \frac{C_\mu}{\sigma_k} \frac{k^2}{\varepsilon} \right) \cdot \left(\nabla \mathbf{U} + (\nabla \mathbf{U})^T \right) \right] + \rho \mathbf{U} \cdot \nabla \mathbf{U} + \nabla P = 0, \tag{2}$$

where C_μ is a model constant equal to 0.09. Turbulence energy and dissipation were found by solving (3) and (4), respectively

$$\rho \frac{\partial k}{\partial t} - \nabla \cdot \left[\left(\mu + \rho \frac{C_\mu}{\sigma_k} \frac{k^2}{\varepsilon} \right) \nabla k \right] + \rho \mathbf{U} \cdot \nabla k = \rho C_\mu \frac{k^2}{\varepsilon} \left(\nabla \mathbf{U} + (\nabla \mathbf{U})^T \right)^2 - \rho \varepsilon, \tag{3}$$

$$\rho \frac{\partial \varepsilon}{\partial t} - \nabla \cdot \left[\left(\mu + \rho \frac{C_\mu}{\sigma_\varepsilon} \frac{k^2}{\varepsilon} \right) \nabla \varepsilon \right] + \rho \mathbf{U} \cdot \nabla \varepsilon = \rho C_{\varepsilon 1} C_\mu k (\nabla \mathbf{U} + (\nabla \mathbf{U})^T)^2 - \rho C_{\varepsilon 2} \frac{\varepsilon^2}{k}, \tag{4}$$

where the model constants $C_{\varepsilon 1}$, $C_{\varepsilon 2}$, σ_k and σ_ε are equal to 0.1256, 1.92, 1.0 and 1.6, respectively. Eqs. (1)–(4) were solved for 2D axial symmetry model using boundary conditions:

- at the inflow:

$$\mathbf{U} = \mathbf{U}_0, \quad k = \left(\frac{3I_T^2}{2} \right) (\mathbf{U}_0 \cdot \mathbf{U}_0), \quad \varepsilon = \frac{C_\mu^{0.75} \left[\left(\frac{3I_T^2}{2} \right) (\mathbf{U}_0 \cdot \mathbf{U}_0) \right]^{1.5}}{L_T}, \tag{5}$$

where turbulent length scale, L_T, was equal to 0.01 and turbulent intensity scale, I_T, was equal to 0.05;

- at the outflow:

$$\mathbf{t} \cdot \mathbf{U} = 0, \mathbf{n} \cdot [-P\mathbf{I} + (\mu + \mu_T)(\nabla \mathbf{U} + (\nabla \mathbf{U})^T)]\mathbf{n} = 0, \quad \mathbf{n} \cdot \nabla k = 0, \mathbf{n} \cdot \nabla \varepsilon = 0. \tag{6}$$

- at the side surface:

$$\mathbf{n} \cdot \mathbf{U} = 0, \mathbf{K} = \left[\frac{\rho C_\mu^{0.25} k^{0.5}}{\ln(\delta_w^+)\kappa} + 5.5 \right] \mathbf{U}, \quad \mathbf{n} \cdot \nabla k = 0, \quad \varepsilon = \frac{C_\mu^{0.75} k^{1.5}}{\kappa \delta_w}, \quad \mathbf{K} = [(\mu + \mu_T)(\nabla \mathbf{U} + (\nabla \mathbf{U})^T)]\mathbf{n}, \quad \delta_w^+ = \frac{\delta_w \rho C_\mu^{0.25} k^{0.5}}{\mu}, \tag{7}$$

where $2\delta_w$ was equal to the step height, h, and the Kármán's constant, κ, is equal to 0.42.

2.2. Mass transfer

A three-dimensional Fickian diffusion model [16] of moisture transfer was applied to simulate the time evolution of the spatial distribution of the local moisture content of carrot during drying:

$$\frac{\partial M}{\partial t} = \nabla \cdot (D \nabla M). \tag{8}$$

A convection-type boundary condition of the following form was applied at the air-product interface

$$-(D \nabla M)|_S = h_m (M_s - M_e); \quad t > 0, \tag{9}$$

where equilibrium moisture content, M_e, was derived from the empirical formulas based on the results of measurements of drying kinetics of carrot cubes.

The initial condition had the following form:

$$M = M_0 = \text{const}; \quad t = 0. \tag{10}$$

2.3. Heat transfer

The model of heat conduction in a carrot cube can be described by the Eq. (11) [17]:

$$\frac{\partial (\rho c_p T)}{\partial t} = \nabla \cdot (\lambda \nabla T). \tag{11}$$

The convection boundary condition in the following form was applied to solve the heat transfer equation:

$$-\lambda\left.\frac{\partial T}{\partial n}\right|_{\mathrm{S}} = h_{\mathrm{T}}(T_{\mathrm{s}} - T_{\mathrm{a}}) - r\left(D\frac{\partial(\rho_{\mathrm{s}}M)}{\partial n}\right), \quad (t > 0), \tag{12}$$

where the term on the left side of the condition (12) refers to heat conducted from the outer surface to the inside of the body, the first term on the right side is heat penetrating from the environment to the solid body by means of convection, and the second term on the right side denotes heat of evaporation. The initial condition has the following form:

$$T = T_0 = \text{const}; \quad t = 0. \tag{13}$$

2.4. Shrinkage

The model of shrinkage was described using Poisson's equation in the form:

$$-\nabla\cdot(\nabla u) = 0, \tag{14}$$

where u is displacement of a point of a body. The boundary condition (displacement of the surface of dried cube) at the air-product interface was assumed as described by the following equation [11]:

$$u|_{\mathrm{S}} = \frac{L_0 - (V)^{\frac{1}{3}}}{2}. \tag{15}$$

Boundary condition (15) describes time dependent displacement of external wall of dried cube.

The initial condition has been assumed in the following form:

$$u = 0; \quad t = 0. \tag{16}$$

The change in volume of a solid particle dried in a spout-fluidized bed is described by linear function of moisture content (17) while the effect of drying temperature is assumed as negligible.

$$\frac{V}{V_0} = a\frac{\overline{M}}{M_0} + (1-a). \tag{17}$$

It can be deducted from Eq. (14) that the displacement, u, of any given point inside dried and shrinking body is a linear function of Cartesian coordinates. And, as a consequence, the displacements of points situated closer to the external surface of dried body are higher than displacement of points situated closer to the sample center.

2.5. Density

The local density at any point inside of carrots particle was calculated by the following formula:

$$\rho = \rho_{\mathrm{w}} + \rho_{\mathrm{s}}, \tag{18}$$

where

$$M = \frac{\rho_{\mathrm{w}}}{\rho_{\mathrm{s}}} \tag{19}$$

and

$$\rho_{\mathrm{s}} = \rho_{0\mathrm{s}}\frac{V_0}{V} \tag{20}$$

which gives

$$\rho = \rho_{0\mathrm{s}}\frac{V_0}{V}(1+M). \tag{21}$$

Eq. (20) was derived based on an analysis of changes in the density of a dry substance while Eq. (21) was derived from Eqs. (18)–(20).

3. The Arbitrary Lagrange–Eulerian formulation

A system of partial differential equations describing simultaneous heat and mass transfer in a single carrot cubes representing a typical particle of the material dried in spout-fluidized bed drier was solved using the weak form of these equations. The Arbitrary Lagrange–Eulerian (ALE) formulation was used to enter a problem with displacing boundaries. In the ALE method, the variables and their test functions were transposed to the original (initial) mesh reflecting the shape of the drying body [18]. The heat transfer Eq. (11) written in the weak form was

$$\int_{\Omega}\rho_{\mathrm{m}}c_p\frac{\partial T}{\partial t}T\_\mathrm{test}\,\mathrm{d}\Omega = \int_{\Omega}\nabla\cdot(\lambda\nabla T)T\_\mathrm{test}\,\mathrm{d}\Omega. \tag{22}$$

In Eq. (22) T is the solution of the differential equation (11) and $T_$test is an arbitrary *test function* satisfying the Eq. (22). By integrating the right side of Eq. (22) by parts (i.e., using Green's formula) one can obtain following equation:

$$\int_{\Omega}\rho_{\mathrm{m}}c_p\frac{\partial T}{\partial t}T\_\mathrm{test}\,\mathrm{d}\Omega = \int_{\Omega}-\lambda\nabla T\cdot\nabla T\_\mathrm{test}\,\mathrm{d}\Omega - \int_{\partial\Omega}\mathbf{n}\cdot(\lambda\nabla T)T\_\mathrm{test}\,\mathrm{d}\partial\Omega. \tag{23}$$

Considering the boundary condition (12), we obtain (24)

$$\int_{\Omega}\rho_{\mathrm{m}}c_p\frac{\partial T}{\partial t}T\_\mathrm{test}\,\mathrm{d}\Omega = \int_{\Omega}-\lambda\nabla T\cdot\nabla T\_\mathrm{test}\,\mathrm{d}\Omega - \int_{\partial\Omega}\mathbf{n}\cdot(h_{\mathrm{T}}(T_{\mathrm{S}} - T_{\mathrm{a}}) - rD\rho\nabla M)\cdot T\_\mathrm{test}\,\mathrm{d}\partial\Omega. \tag{24}$$

Mass transfer Eq. (8) in its weak form obtains the form (25)

$$\int_{\Omega}\rho\frac{\partial M}{\partial t}M\_\mathrm{test}\,\mathrm{d}\Omega = \int_{\Omega}-D\rho\nabla M\cdot\nabla M\_\mathrm{test}\,\mathrm{d}\Omega - \int_{\partial\Omega}\mathbf{n}\cdot h_{\mathrm{m}}(M_{\mathrm{S}} - M_{\mathrm{e}})\cdot M\_\mathrm{test}\,\mathrm{d}\partial\Omega, \tag{25}$$

while the shrinkage Eq. (14) the form (26)

$$\int_{\Omega}-\nabla u\cdot\nabla u\_\mathrm{test}\,\mathrm{d}\Omega - \int_{\partial\Omega}\mathbf{n}\cdot u\_\mathrm{test}\,\mathrm{d}\partial\Omega = 0. \tag{26}$$

The equations were solved on the original mesh, and the results were transferred to a movable mesh. The ALE method may be applied for large-scale deformation modeling [19,20]. An attempt to describe the drying processes of shrinking bodies, taking into account the stress distribution in the material, leads to quite complicated mathematical models [21]. If the information on stress evolution during drying is disregarded, then the application of the ALE formulation provides relatively simple models.

4. Experiments

Experiments were conducted to validate the simulation results of changes in carrot moisture content and temperature during drying in a spout-fluidized bed drier.

Experiments with carrot drying were conducted using a spout-fluidized bed drier as shown on Fig. 1. A pilot-scale dryer with the conical section underneath (0.25 m in height), was a vertical cylindrical column (0.2 m diameter and 1 m height) equipped with a supporting grid, as a gas distributor. Air was supplied to the conical section by a pipe 0.065 m in diameter. The cone part of the drying chamber was made of stainless steel and the cylinder part was made from perspex. Hot air was distributed to the bottom of the chamber through an air distributor plate. Air was heated by electric heaters with a total capacity of 15 kW. The inlet air temperatures were automatically controlled by a PDI temperature controller, with an accuracy of ±1 °C. Temperatures were measured by J-type thermocouples with an accuracy of ±1 °C. Air velocity was measured using an LCA30VA (Test-Therm, Cracow, Poland) anemometer with an accuracy of ±5%. The moisture content of the sample during drying was determined by weighing the sample together with the drying chamber for about 5 s every 10 min using an AXIS B15W electronic balance. The accuracy of the weighing was ±1 g.

The carrots (*Daucus carota cv Macon F1*) were used as the drying product. In order to ensure reproducible results, the material was obtained from the experimental plots of the Agricultural Research Institute in Skierniewice in Poland, and kept refrigerated at 3 °C for one month. After stabilizing at room temperature prior to use, the carrots were washed, peeled, cut into 10 mm cubes and dried using a spout-fluidized bed drier. The initial moisture content of carrots (8.2 kg kg^{-1}) was determined by drying in a laboratory dryer at 105 °C for 24 h. The experiments were carried out using four different operating temperatures of 60, 70, 80 and 90 °C. The inlet air temperature, the air temperature in the bed and material temperature were registered by a PC with a 30-s time step. A temperature controller was used for regulating the temperature of drying air within ±3 °C. The temperature of the center of the sample was measured with a thermocouple fixed near the geometric center of one of the dried carrot cubes set about 10 cm above the supporting grid. Several samples for each run were taken during drying to measure the effect of operating conditions on material shrinkage. Indirect measurements of volume shrinkage were applied [22].

The initial height of stationary layer of cut carrots was about 0.1 ± 0.01 m. Since a significant shrinkage took place during drying process, the demands of the air-flow required to maintain a fountain at a constant height were diminishing. Therefore, the experiments were conducted under a step-wise decreasing air flow velocity.

5. Results and discussion

5.1. Calculation of the air velocity profiles

Computer simulations were performed using *COMSOL MULTIPHYSICS* 3.3a (Comsol AB, Sweden) with the *CHEMICAL ENGINEERING MODULE* and *HEAT TRANSFER MODULE* extensions. The packages used numerical algorithms based on the finite element method.

In order to perform computer simulations of heat and mass transfer in carrot cubes during drying in a spout-fluidized bed drier, the velocity of the air flowing round a single cube should be known. The value of this quantity was estimated using a model (1)–(7) describing the motion of the air through the empty drying chamber and was calculated as the velocity of the air averaged over the domain in which the material resided during drying, and was then used for calculation of heat and mass transfer coefficients based on Eqs. (32) and (33). The domain containing most of the material during drying was axi-symmetric and its axial section was marked as polygon ABCD, as shown in Fig. 2a. The AB segment of the line as marked in Fig. 2a is placed at the same level of the cylinder as the grid supporting the dried material.

The geometry of the drying chamber, process parameters and the physical parameters of the material used during simulations were the same as those observed during the experiments. The temperature, viscosity and density of the air used during the simulation were 80 °C, 2×10^{-5} Pa s and 1.06 kg m^{-3}, respectively. The measured inlet air velocity was 41 m s^{-1} during the initial phase of drying and 27 m s^{-1} in the final drying phase. Fig. 2a also shows simulated air velocity profiles on the region of axial section drying chamber which is located close to the orifice supporting the material. It can be found from Fig. 2a that the velocity of the air averaged over the domain in which the material resided during drying was close to 41 m s^{-1}, and that value was used during simulation.

5.2. Experimental validation

Coupled heat and mass transfer processes accompanied by the shrinkage of the material during drying were calculated using Cartesian coordinates OXYZ, in which point O was fixed to the center of a carrot cube. For simulation purposes, in order to reduce the number of finite elements applied, the symmetries of a dried particle were used. As OXY, OYZ and OXZ were the symmetry planes of a cube,

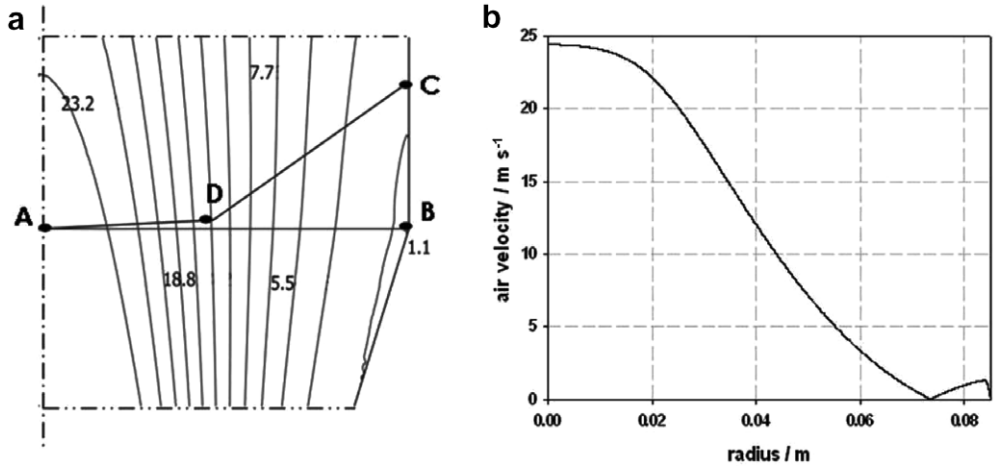

Fig. 2. Profiles of air velocity at 80 °C: (a) fragment of section along the symmetry axis of the cylinder and (b) section perpendicular to an axis along the AB segment of the line.

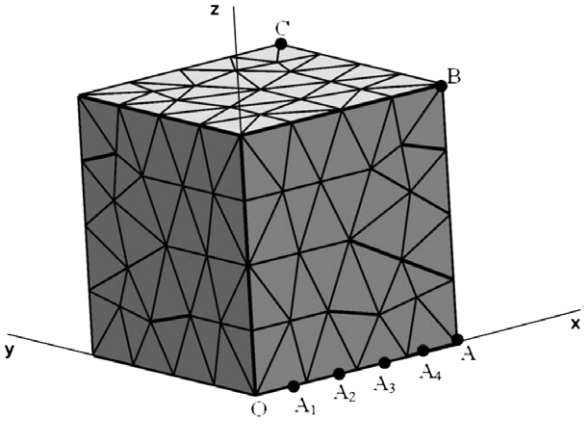

Fig. 3. Meshing of 1/8 of part of sample with a used *regular* refinement method at 559 number of elements distribution.

only a quarter of the upper half of a cube was used during simulation, as can be seen in Fig. 3. On the same figure three characteristic points inside of a carrot cube were selected: point A – located in the middle of one of the sides of a cube; point B – located in the middle of one of the ages of the cube, and point C – located along one of the cube's vertices. Furthermore, Fig. 3 shows additional four points: A_1, A_2, A_3, A_4, located on the interval OA in such a way that the interval is divided by those points into five intervals of equal length. Before the simulation, the dried carrot cube was divided into 559 finite elements using the *regular* refinement method and the model was solved for 5558 degrees of freedom. The Laplace smoothing method was used during simulation. The model parameters and thermo-physical properties of gas and solids determined experimentally or calculated based on the results presented in professional scientific literature are presented in Table 1. All the Cartesian co-ordinates used were referenced to the original (initial) shape of a sample.

Typical changes in the mean value of water content, as well as the local error of estimation calculated for drying of carrot cubes (in %) are shown in Fig. 4. It was observed that the shapes of characteristics received for all temperatures applied were similar. Therefore, Fig. 4 shows only the characteristics received for drying at 60 °C and 90 °C. It can be observed in Fig. 4 that the predicted moisture content during drying decreased faster than the measured moisture content. Three phases of drying were distinguished according to behavior of changes in percent local error of estimation. The percent local error of estimation of moisture content during the initial phase of carrots drying at 60 °C was relatively low and its value oscillated in a range between −10% and +10%, while for drying at 90 °C the oscillations of the error ranged between −5% and 10%. The material lost a significant amount of water during the initial phase of drying – moisture content decreased from the initial value of ca. 8.2 kg kg^{-1} to ca. 2 kg kg^{-1}. During the second phase of drying, the percent local error of estimation increased rapidly to receive a maximum of 82% for air temperature 60 °C and 98% for 90 °C. During the third phase of drying, the percent local error of estimation decreased monotonically to reach 30% for drying at 60 °C and 59% for drying at 90 °C. The measured and predicted moisture contents in carrots after 180 min of drying at 60 °C were 0.132 kg kg^{-1} and 0.094 kg kg^{-1}, respectively, while 0.082 kg kg^{-1} and 0.034 kg kg^{-1}, respectively, after 120 min of drying at 90 °C. The acceptable agreement between the measured and predicted values can be noted for the initial phase and final phases of drying when the shrinkage of the material and the moisture loss were very pronounced, but the model tended to underestimation the moisture content in carrots during the second phase of drying. The discrepancies between measured and predicted values of moisture content observed for the second drying phase may have been caused by the linear type of the shrinkage Eq. (14) which describes only isotropic deformations of the being dried materials. The additional errors could have been caused by the assumptions made for formulating Eq. (21). The assumptions of porous and

Table 1
Thermo-physical properties of air and carrots used in model solutions

Specific heat of carrots [24]:

$$c_p = 1000(1.4 + 3.22 \cdot X) \tag{27}$$

Thermal conductivity of carrots [24]:

$$k = 0.148 + 0.493 \cdot X \tag{28}$$

Sorption heat [25]:

$$r = 2889.4 \times 10^3 \left(1 - \frac{(273+T)}{647.13}\right)^{(0.3199 - 3.276\times10^{-4}(273+T) + 6.1596\times10^{-7}(273+T)^2)} \tag{29}$$

Effective mass diffusion coefficient in gas phase [26]:

$$D_{AB} = 1.87 \times 10^{-10} \frac{(T_f + 273)^{2.072}}{P}; \quad \text{where } T_f = \frac{T_S + T_a}{2}; \quad P = 1 \text{ atm} \tag{30}$$

The Nusselt, Prandtl, Sherwood, Schmidt and Reynolds numbers [27]:

$$Nu = \frac{h_T d_E}{\lambda}; \quad Pr = \frac{c_{p_{air}} \eta_{air}}{\lambda}; \quad Sh = \frac{h_m d_E}{D_{AB}}; \quad Sc = \frac{\eta_{air}}{\rho_{air} D_{AB}}; \quad Re = \frac{d_E v \rho_{air}}{\eta_{air}} \tag{31}$$

Correlation equation used for evaluation of heat transfer coefficient [27]:

$$Nu = 2.0 + 0.6(Pr)^{1/3}(Re)^{1/2} \tag{32}$$

Correlation equation used for evaluation of mass transfer coefficient [27]:

$$Sh = 2.0 + 0.6(Sc)^{1/3}(Re)^{1/2} \tag{33}$$

Parameters of air [28]:

$$\rho_{air} = -3.510101 \times 10^{-8} T_f^3 + 1.583982684 \times 10^{-5} T_f^2 - 4.6995202202 \times 10^{-3} T_f + 1.29213571428571; \quad (10\,^\circ\text{C} < T_f < 80\,^\circ\text{C}) \tag{34}$$

$$\mu_{air} = 1.7676768 \times 10^{-13} T_f^3 - 5.541125541 \times 10^{-11} T_f^2 + 4.983297258297 \times 10^{-8} T_f + 17.1964285714285 \times 10^{-6}; \quad (10\,^\circ\text{C} < T_f < 80\,^\circ\text{C}) \tag{35}$$

$$\lambda_{air} = 6.8181818 \times 10^{-10} T_f^3 - 1.474025974 \times 10^{-7} T_f^2 + 8.029112554113 \times 10^{-5} T_f + 0.0240835714285714; \quad (10\,^\circ\text{C} < T_f < 80\,^\circ C) \tag{36}$$

$$Pr = -2.272727 \times 10^{-8} T_f^3 + 4.1991342 \times 10^{-6} T_f^2 - 3.5335497835 \times 10^{-4} T_f + 0.719; \quad (10\,^\circ C < T_f < 80\,^\circ\text{C}) \tag{37}$$

Effective moisture diffusivity of carrot [29,30]:

$$D = 2.779 \times 10^{-4} \exp\left(-0,97 - \frac{3459.8}{T} + 0.059M\right) \tag{38}$$

The diameter of a sphere equivalent to a particle of volume[31]:

$$d_E = \sqrt[3]{6\frac{V_E}{\pi}} \tag{39}$$

homogenous structure of the material seem to be true for non-organic samples but they are not necessarily true for organic matter which is colloidal, capillary and, in nature, shrinks non-uniformly.

In order to improve the ability of the model to predict the changes in temperature of dried carrots, a very simple test of sensitivity of the model on the changes in heat transfer coefficient was performed. Figs. 5 and 6 show measured and predicted changes in temperature of the central point of the sample. Both the measured and simulated results of changes in temperature at the central point of carrot sample during drying, as presented in Figs. 5 and 6, were obtained for three different values of heat transfer coefficient: i.e. the first one, h_T, was derived from Eq. (32), the

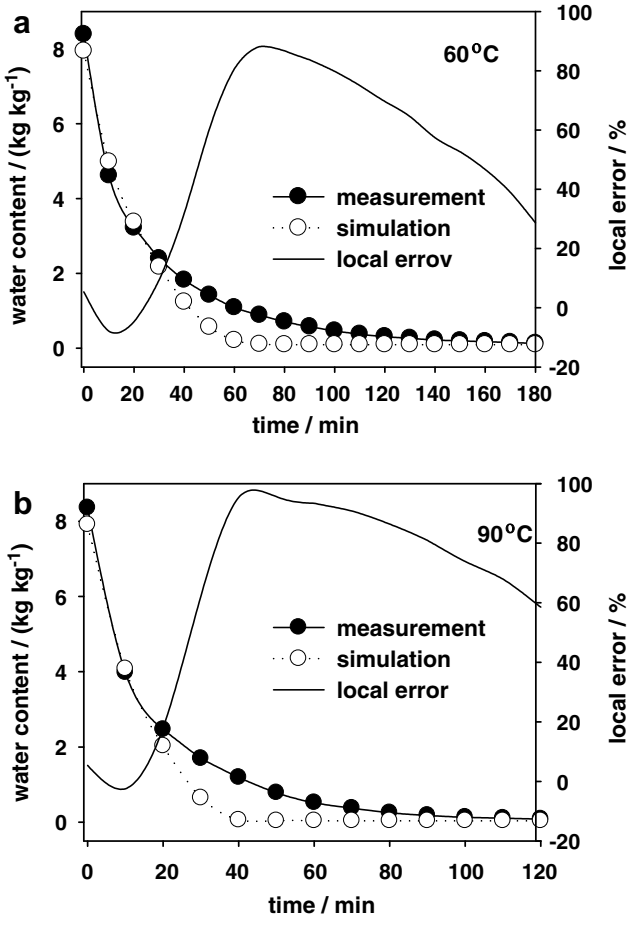

Fig. 4. Changes in water content in carrots during drying and percent local error of prediction: (a) drying at 60 °C and (b) drying at 90 °C.

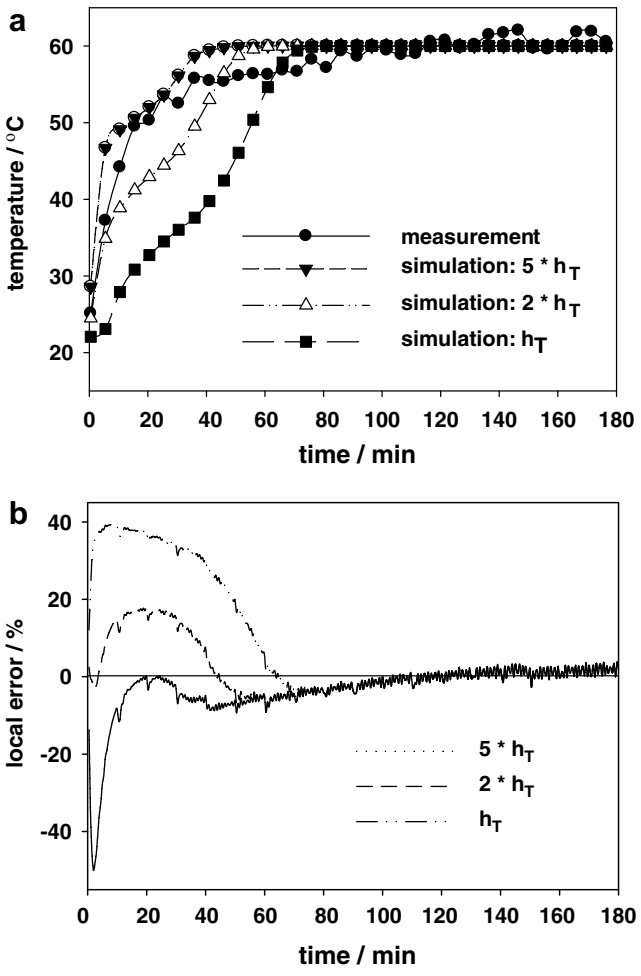

Fig. 5. Measured and predicted changes in temperature at the center point of a single carrot cube dried at 60 °C, (a). Local percent error of prediction, (b).

second one, 2^*h_T, was duplication of the first one and the third one, 5^*h_T, was fivefold of the first one. The air velocity around the dried carrot cube used in Eq. (32) was assumed to equal 4 m s^{-1}, which is in the agreement with the results of simulated air velocity profiles in a drying chamber as shown in Fig. 2. As can be seen in Figs. 5 and 6, the best prediction of the sample temperature was received using the second variant of heat transfer coefficient. It was also found that the changes in heat transfer coefficient, as applied in this study, did not affect the prediction of changes in the moisture content in dried carrots. The following explanation of differences observed between measured and predicted temperatures in dried carrot cubes can be given. In order to measure the instantaneous particle temperature, one sample carrot was fixed about 10 cm above the supporting grid and its center temperature was measured, while in the real case of spouted-fluid bed, particles (carrots) moves up and then rain down. On the other hand the difference between the measured temperatures and predicted ones in the case of $1 \times h_T$ may not be caused by a low heat transfer coefficient calculated from Eq. (32). On the contrary, the difference may be caused by the thermal conductivity of carrots calculated from the empirical Eq. (28), which may be lower than practical one.

The predicted results of both moisture content and temperature of the sample indicate that if a very high accuracy of moisture content and temperature prediction is not a crucial element of investigation into the heat and mass transfer during drying of particulate materials in a spout-fluidized bed drier, then the model can be successfully applied for describing moisture content, temperature and deformation of dried particles.

5.3. Simulation of shrinkage, moisture content and temperatures of dried carrots

Simulated displacements of selected points (as described in Fig. 3) of a shrinking carrot cube dried at 60 °C are shown in Fig. 7. It can be observed on Fig. 7 that the external layers of a dried cube are characterized by much greater deformations than the layers located near center of a particle. According to the model of shrinkage described by Eqs. (14)–(17) deformation of any region of a dried body occurs immediately after the start of the process. It was a simplification because it is expected that points near the

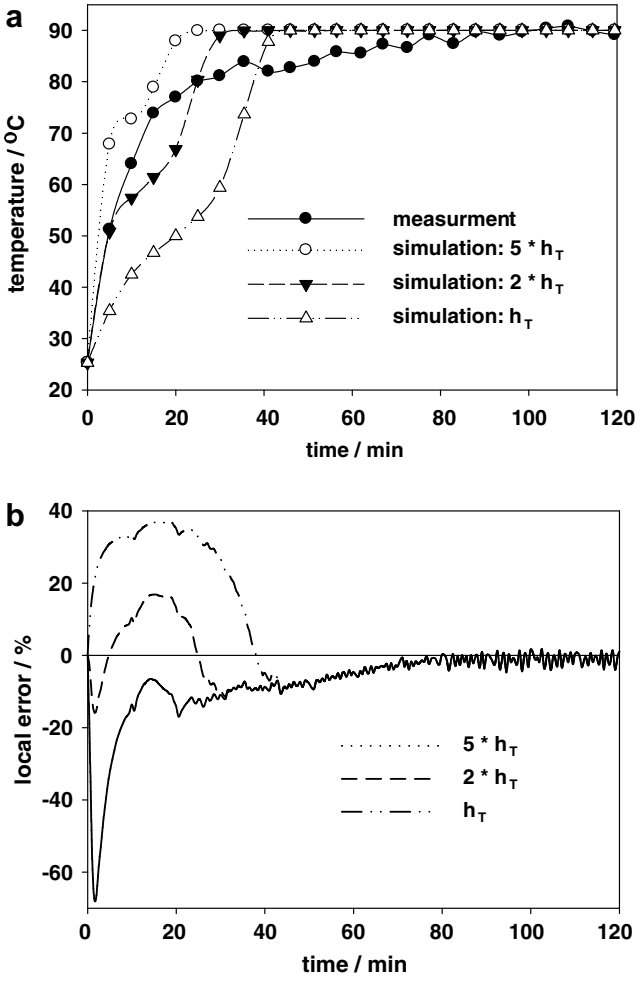

Fig. 6. Measured and predicted changes in temperature of the center point of a single carrot cube dried at 90 °C, (a). Local percent error of prediction, (b).

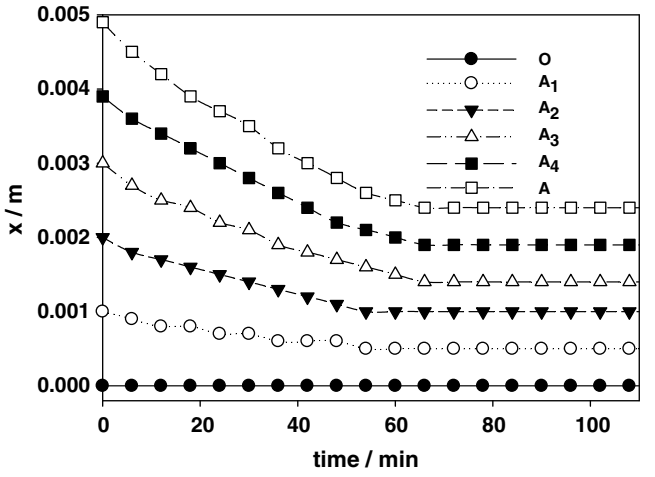

Fig. 7. Simulated displacements of selected points of shrinking carrot cube dried at 60 °C. Points A_1, A_2, A_3, and A_4 divide the interval OA into five intervals of equal length (see Fig. 3).

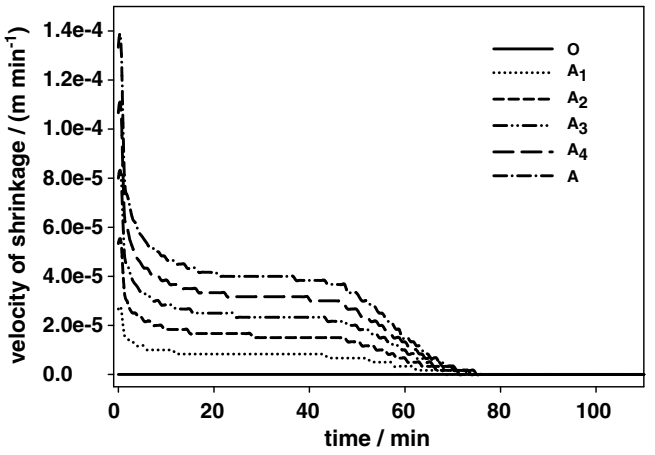

Fig. 8. Rate of deformation simulated at selected points of carrot cubes inside the specimen during drying at 60 °C. Points A_1, A_2, A_3, and A_4 divide the interval OA into five intervals of equal length (see Fig. 3).

center of a sample do not move immediately after the start of the process [23]. However, if it is considered that heat and mass transfer processes are very intensive (as during drying in a spout-fluidized bed) this simplification does not influence the results significantly.

Fig. 8 shows the rate of deformation of a dried carrot cube at several points on segment OA of the specimen (see Fig. 3) which occurred during drying at 60 °C. The profiles of the rate of deformation shown in Fig. 8 indicated the existence of the initial phase of simulated drying process characterized by the steep decrease in velocity of displacement of given points inside the specimen followed by the phase of almost constant rate of deformation. The final phase of the process was characterized by slow decrease of the deformation velocity. This means that the rate of deformation of carrot cubes dried in a spout-fluidized bed drier was non-linear vs. time and its magnitude depended on the position inside the particle being dried.

Changes in simulated local values of water content inside the dried carrot cube at several points on segment OA of the specimen (see Fig. 3) were shown in Fig. 9. It can be seen in Fig. 9 that the surface of the cube (point A) achieved its equilibrium water content almost at the very beginning of the drying process. It means that the external resistances of drying were low from the beginning of drying. On the same figure, it can be observed that the higher the distance of the point being analyzed from center of the dried particle, the lower the local moisture content was at that point. The above observations are in agreement with the observations of Zielinska and Markowski [5] who found that heat and mass transfer coefficients during spout-fluidized bed drying of carrot cubes were in the ranges from 13 to 38 $W\,m^{-2}\,K^{-1}$ and from 7 to 17 $m\,s^{-1}$, respectively, while the Biot number for the mass transfer exceeded the value of 100 quickly – which means that internal resistances in mass transfer had an crucial influence on the carrot cube drying process in a spout-fluidized bed drier. The sudden increase of moisture content in the internal points of dried

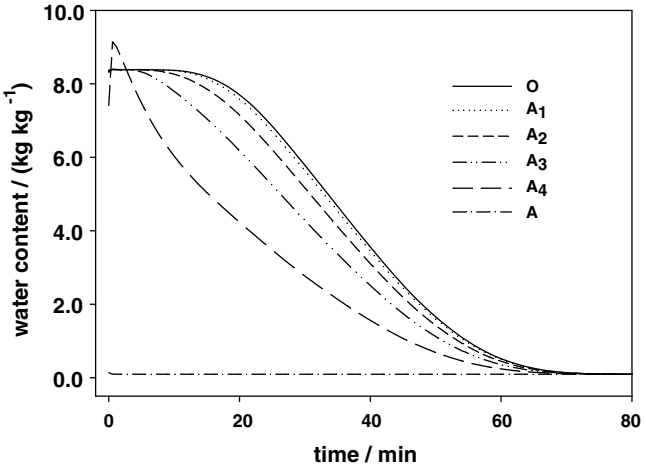

Fig. 9. Changes in local water content in the carrot cube during drying at 60 °C. Points A_1, A_2, A_3, and A_4 divide the interval OA into five intervals of equal length (see Fig. 3).

cube at the initial stage of drying, which exceeds the initial moisture contents of carrots can be explained by the shrinkage of the material during drying.

Changes in temperatures simulated at selected points of a sample dried at 60 °C are shown in Fig. 10. After a very short phase of a steep decrease, the simulated temperatures at all points of the cubes raised to reach a level close to the temperature of the air. It can be observed that the temperatures simulated at the middle point of the edge of a cube (point B in Fig. 3) and at its the vertex (point C in Fig. 3) were lower than the temperature of each internal point situated on the segments OB and OC, with highest temperature received at point O, as can be seen in Fig. 10b and c. This situation is typical for the process of heating a solid cube by conduction under the absence of a coupled mass transfer of liquid moisture inside the solid and moisture vaporization at the cube's surface. When the heating is accompanied by mass transfer (liquid moisture diffusion inside the body and vaporization at its external surface) the situation is different – as can be observed in Fig. 10a. It can be noted in Fig. 10a that the temperature of a cube simulated at the middle point of the lateral face of a cube (point A on Fig. 3) was lower than the temperature at the cube's center. The energy consumption necessary for intensive moisture vaporization at point A of a cube in comparison with the relatively low intensity of moisture vaporization at points B and C can be an explanation of the above phenomena. The sudden decrease of the sample temperature at the initial stage of drying observed in Fig. 10 can be explained by intensive moisture evaporation during the initial stage of the drying.

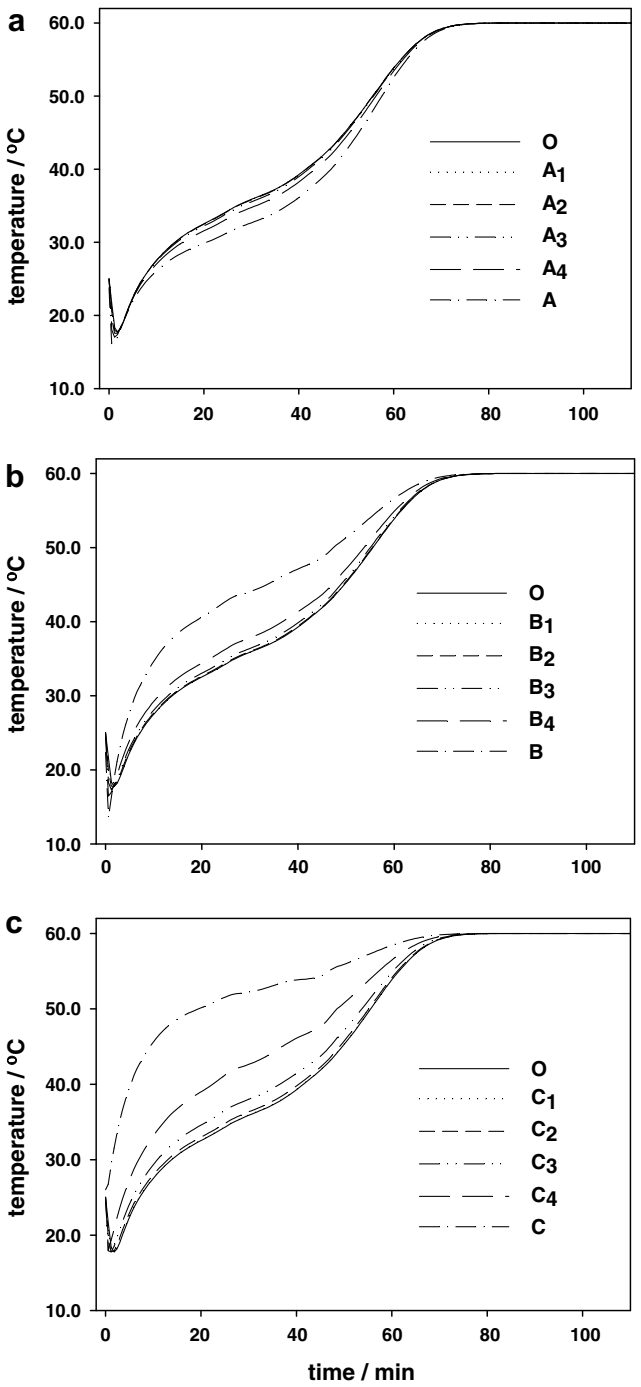

Fig. 10. Simulated changes in temperatures at selected points of a sample dried at 60 °C: (a) points A_1, A_2, A_3, and A_4 divide the interval OA into five intervals of equal length (see Fig. 3); (b) points B_1, B_2, B_3, and B_4 divide the interval OB into five intervals of equal length and (c) points C_1, C_2, C_3, and C_4, divide the interval OB into five intervals of equal length.

6. Concluding remarks

This paper presents the mathematical model of drying kinetics of carrots dried in a spout-fluidized bed drier. The study was carried out using a numerical solution of a system of three linked equations. The Arbitrary Lagrange–Eulerian (ALE) method was applied to enter the problem with moving boundaries. It was found that the velocity of the air averaged in the domain containing carrot cubes during drying was ca. 4 m s^{-1}. Three phases

of drying were distinguished according to behavior of changes in percent local error of estimation: i.e. the first phase described by low error of prediction, the second phase characterized by an increase in error of moisture content prediction followed by the phase of decreasing error of moisture content prediction. A simple test of sensitivity of the model to the changes in heat transfer coefficient was performed in order to improve the ability of the model to predict the changes in the temperature of the dried carrots. It was found that the highest accuracy of carrot temperature prediction was observed if the value of heat transfer coefficient applied during simulation was two times higher than the value calculated based on Eq. (32). It was also found that the external layers of dried and shrinking carrot cubes were characterized by much greater deformations than the layers located near the center of a particle. The results of the simulation showed that the rate of deformation of convection dried carrot cubes was non-linear vs. time and its magnitude depended on the position inside the particle being dried and that the external resistances of drying were low from the beginning of drying. It was also observed from the simulation results that after a very short phase of steep decrease, the simulated temperatures at all points of the cubes rose to reach a level close to the temperature of the air, however, the temperatures simulated in the middle of the wall of a cube increased slower than at other points. The results obtained for both moisture content and temperature of the sample indicate that if a very high accuracy of prediction of moisture content and temperature of the bed of a particulate material dried in a spout-fluidized-bed drier is not a crucial element of investigation, then the model can be successfully applied as a tool describing moisture content, temperature and the deformation of dried particles.

In a spouting bed the disperse phase concentration has a pronounced inhomogeneity which in principle should affect gas phase distribution as well as the heat and mass transfer processes. In the present model differences in the coefficients of heat and mass transfer in the core and the periphery zone are not taken into account. This is a limitation of the model that needs to be examined in further research. Further experimental studies are needed to verify definitively the validity of the one-phase model of hydrodynamics in the description of an inherently two-phase flow with a high concentration of the dispersed phase. This is further complicated by the simultaneous heat and mass transfer processes and the significant shrinkage phenomenon occurring in the dispersed phase.

References

[1] M.S. Hatamipour, D. Mowla, Shrinkage of carrots during drying in an inert medium fluidized bed, J. Food Eng. 55 (2002) 247–252.

[2] A. Reyes, P.I. Alvarez, F.H. Marquardt, Drying of carrots in a fluidized bed. I. Effects of drying conditions and modelling, Dry. Technol. 20 (7) (2002) 1463–1483.

[3] A. Mhimid, S. Ben Nasrallah, J.P. Fohr, Heat and mass transfer during drying of granular products simulation with convective and conductive boundary conditions, Int. J. Heat Mass Transfer 43 (2000) 2779–2791.

[4] W. Zhonghua, A.S. Mujumdar, Simulation of the hydrodynamics and drying in a spouted bed dryer, Dry. Technol. 25 (1) (2007) 59–74.

[5] M. Zielinska, M. Markowski, Drying behavior of carrots dried in a spout-fluidized bed dryer, Dry. Technol. 25 (2007) 261–270.

[6] K.M. Waananen, J.B. Litchfield, M.R. Okos, Classification of drying models for porous solids, Dry. Technol. 11 (1) (1993) 1–40.

[7] M.E. Katekawa, M.A. Silva, A review of drying models including shrinkage effects, Dry. Technol. 24 (1) (2006) 5–20.

[8] L. Mayor, A.M. Sereno, Modelling shrinkage during convective drying of food materials: a review, J. Food Eng. 61 (2004) 373–386.

[9] J.E. Lozano, E. Rotstein, M.J. Urbican, Shrinkage, porosity and bulk density of foodstaffs at changing moisture content, J. Food Sci. 48 (1983) 1497–1502.

[10] N.P. Zogzas, Z.B. Maroulis, D. Marinos-Kouris, Densities, shrinkage and porosity of some vegetables during air drying, Dry. Technol. 12 (7) (1994) 1653–1666.

[11] I. Białobrzewski, Determination of the heat transfer coefficient by inverse problem formulation during celery root drying, J. Food Eng. 74 (2006) 383–391.

[12] I. Białobrzewski, Determination of the mass transfer coefficient during hot-air-drying of celery root, J. Food Eng. 78 (2006) 1388–1396.

[13] J. Zhang, A.K. Datta, Some consideration in modeling of moisture transport in heating of hygroscopic materials, Dry. Technol. 22 (8) (2004) 1983–2008.

[14] E. Balsa-Canto, A.A. Alonso, J.R. Banga, A novel, efficient and reliable method for thermal process design and optimization. Part I: theory, J. Food Eng. 52 (2002) 227–234.

[15] E. Balsa-Canto, A.A. Alonso, J.R. Banga, A novel, efficient and reliable method for thermal process design and optimization. Part II: applications, J. Food Eng. 52 (2002) 235–247.

[16] J. Crank, The Mathematics of Diffusion, second ed., Oxford University Press, New York, 1975.

[17] H.S. Carslaw, J.C. Jaeger, Conductions of Head in Solids, second ed., Oxford University Press, New York, 1986.

[18] T. Belytschko, W.K. Liu, B. Moran, Nonlinear Finite Elements for Continua and Structures, John Wiley and Sons, Ltd., New York, 2000.

[19] P.L. Tallec, J. Mouro, Fluid structure interaction with large structural displacements, Comput. Methods Appl. Mech. Eng. 190 (2001) 3039–3067.

[20] S. Tanaka, K. Kashiyama, ALE finite element method for FSI problems with free surface using mesh re-generation method based on background mesh, Int. J. Comput. Fluid Dyn. 20 (3–4) (2006) 229–236.

[21] D. Mihoubi, F. Zagrouba, J. Vaxelaire, A. Bellagi, M. Roques, Transfer phenomena during the drying of a shrinkable product: modeling and simulation, Dry. Technol. 22 (1–2) (2004) 91–109.

[22] M. Zielinska, The influence of selected parameters on the kinetics of spout-fluidized bed drying and quality of dried carrot. Ph.D. Thesis, Olsztyn, 2005 (in Polish).

[23] I. Białobrzewski, Simulation of changes in the density of an apple slab during drying, Int. Commun. Heat Mass Transfer 33 (2006) 880–888.

[24] V.E. Sweat, in: M.A. Rao, S.S.H. Rizvi (Eds.), Thermal Properties of Foods. Engineering Properties of Foods, second ed., Marcel Dekker, Inc., New York, 1995.

[25] R.H. Perry, C.H. Chilton, Chemical Engineering Handbook, McGraw-Hill, Kogakusha, 1973.

[26] Y.A. Cengel, Heat and Mass Transfer – A Practical Approach, third ed., McGraw-Hill, USA, 2006.

[27] R.B. Bird, W.E. Steward, E.N. Lightfood, Transport Phenomena, John Wiley & Sons, Inc., New York, 2002.

[28] R. Islam, A.S. Mujumdar, Simulation of liquid diffusion-controlled drying of shrinking thin slabs subjected to multiple heat sources, Dry. Technol. 21 (2003) 413–438.
[29] A. Mulet, A. Berna, C. Rosello, F. Pinga, Drying of carrots: II – Evaluation of drying models, Dry. Technol. 7 (1989) 641–661.
[30] S. Simal, E. Deya, M. Frau, C. Rossello, Simple modeling of air drying curves of fresh and osmotically pre-dehydrated apple cubes, J. Food Eng. 33 (1997) 139–150.
[31] M. Serwinski, Principles of Chemical Process Engineering, first ed., WNT, Warsaw, 1971 (in Polish).